How lasers can push silicon–graphite anodes towards next-generation battery

W. Pfleging*, Y. Zheng

Karlsruhe Institute of Technology, IAM-AWP, P.O. Box 3640, 76021 Karlsruhe, Germany

ABSTRACT

Graphite anode material is commonly used in lithium-ion batteries. Due to the demand for a significantly increased energy density for xEVs (electromotive vehicles), there is worldwide a strong effort to add nano-sized silicon particles to composite graphite electrodes. Silicon has the benefit to provide one order of magnitude higher gravimetrical energy density than graphite. However, a bottleneck of silicon is its huge volume expansion of about 300 % during electrochemical cycling which induces high compressive stress and subsequent film delamination, crack formation, and finally degradation of electrochemical cells. In this study, thick film graphite, silicon, and silicon–graphite composite electrodes were developed and subsequently ultrafast laser structured in order to reduce compressive stress during electrochemical cycling and diffusion overpotential. The latter one is a critical issue at elevated power densities and for high film thicknesses, i.e., mass loading. By laser ablation, grid structures were introduced into the electrodes and 3D elemental mapping could demonstrate that new lithium-ion diffusion pathways arise along the structure's sidewalls and are activated with increasing power densities. It was successfully shown that laser structured electrodes benefit from a homogenous lithiation, reduced compressive stress, and an overall improved electrochemical performance in comparison to unstructured electrodes. A reduced mechanical and chemical cell degradation was achieved with structured electrodes in comparison to unstructured ones and design rules for silicon–graphite electrode architectures were derived. Laser structuring of electrodes offers a new manufacturing tool for next-generation battery production to overcome current limitations in electrode design and cell performance.

Keywords: ultrafast laser structuring, silicon, graphite, lithium-ion battery, 3D battery, laser-induced breakdown spectroscopy

1. INTRODUCTION

Lithium-ion batteries (LIBs) have become a common and important energy storage device for hybrid and electric vehicles (xEV) [1]. The production cost of LIBs per kilowatt-hour was USD 764 in 2009–2010 and could already be reduced to USD 111 in 2020 [2, 3]. A further reduced cost of USD 92 was forecasted in 2025 [4]. The further development of xEV is closely linked to the next generation of LIBs, which are characterized by an increased power and energy density [5]. At cell level, energy densities of about 350–500 Wh/kg are targeted [6]. Furthermore, short charging times and an extended driving range (>600 km) have been aimed for future xEV. For this purpose, further material and electrode architecture development is necessary. Silicon (Si) has been considered as a next-generation anode material due to its theoretical capacity, which is almost one order of magnitude higher than that of the commonly used graphite (372 mAh/g) [7]. However, during battery operation silicon undergoes an enormous volume change of up to 300%, which is a well-known bottleneck for the commercialization of silicon-based anodes. Particle cracking occurs during volume changes and leads to pulverization, electrical insulation of the silicon, and film delamination [8]. Therefore, a significant improvement of chemical and mechanical integrity of Si-based anodes is of fundamental interest for the establishment of next-generation batteries with enhanced lifetime, cycling stability, and capacity retention [9]. For this purpose, a combined utilization of graphite and Si powders within a 3D electrode architecture seems to be a promising approach. Graphite has a low specific capacity but can provide improved volumetric energy density, cycle stability, and a long cycle lifetime (> 500 cycles); while silicon contributes to the increased specific capacity at anode side [10, 11]. 3D electrode architectures can be easily

* wilhelm.pfleging@kit.edu; phone +49 721 608 22889; http://www.iam.kit.edu/awp/165.php

achieved by ultrafast laser structuring which so far has been successfully implemented on lab scale [12, 13]. Mechanical tensions within the silicon–graphite (Si/C) electrodes can be significantly reduced by introducing 3D electrode architectures while an improvement in rate capability, cycle stability, and cell lifetime can be gained [13]. In this work, the lithium concentration profiles in laser structured and unstructured Si/C electrodes were studied as function of C-Rate at lithiated and delithiated states. The impact of 3D electrode architecture on cell performance and cell degradation mechanisms will be discussed. For this purpose, laser-induced breakdown spectroscopy was employed and electrochemical analytics of Si and Si/C electrodes were performed and evaluated.

2. EXPERIMENTAL

2.1 Battery Materials

The silicon–graphite electrodes consisting of 10 wt% silicon were fabricated for the studies. The total mass fraction of silicon and graphite was kept to 80 wt%. Nano-sized Si particles with an average particle size of 150 nm (2W iTech, LLC, San Diego, CA, USA) were used. Silicon particles were mixed with flake-like graphite particles (D_{50} = 15.26 µm, Targray, Kirkland, QC, Canada) and carbon black (Timcal Super C65, MTI Corporation, New York, NY, USA) in pre-prepared sodium carboxymethyl cellulose (Na-CMC, MTI Corporation, Richmond, CA, USA) solution. A planetary ball milling machine (Pulverisette 7 premium line, Fritsch GmbH, Idar-Oberstein, Germany) enables the achievement of a homogenous slurry. Finally, 5 wt% styrene-butadiene rubber (SBR, MTI Corporation, Richmond, CA, USA) was added at the end of the mixing process. The slurry was coated via tape casting on a nickel-coated copper current collector (Targray, Kirkland, QC, Canada). Afterwards, the electrode was dried at room temperature for 2.5 hours. Prior to laser structuring, the electrode was calendered using a hot rolling press machine (HR01 Hot Rolling Machine, MTI Corporation, Richmond, CA, USA). Finally, the prepared electrodes reveal a porosity of about 42 %.

2.2 Laser Structuring

A laser materials processing system (PS450-TO, Optec, Frameries, Belgium) equipped with a femtosecond laser (Tangerine, Amplitude Systèmes, Bordeaux, France) was used for laser cutting of electrodes and to create 3D structures on the surfaces of the electrodes. The femtosecond laser operates at a fundamental wavelength of 1030 nm with a pulse duration of 350 fs. The pulse repetition rates of 200 kHz and 500 kHz were applied for cutting and structuring, respectively. With respect to isotropic volume expansions of silicon during battery operation, grid structures with a pitch of 100 µm and 300 µm were generated in the manufactured electrodes.

2.3 Battery Operation

Coin cells of type CR2032 (MTI Corporation, Richmond, CA, USA) were used to characterize the electrochemical properties of the laser-structured and unstructured electrodes. Cell assembly was performed in a glove box filled with argon (LABmaster SP, MBraun Inertgas-Systeme GmbH, Munich, Germany) in a high-purity atmosphere (O_2 < 0.1 ppm, H_2O < 0.1 ppm). The circular electrodes examined have a diameter of 12 mm. Lithium foil (Sigma Aldrich, St. Louis, MO, USA) with a thickness of 250 µm and a diameter of 11 mm was applied as counter electrode. A glass fiber separator with a diameter of 15 mm (GF/A filter, thickness 260 µm, Whatman, Maidstone, UK) served as an electrical insulator between the electrodes. The used electrolyte (LP57, Merck AG, Darmstadt, Germany) consists of a 1.3 mol/L lithium hexafluorophosphate ($LiPF_6$) in ethylene carbonate (EC) and ethyl methyl carbonate (EMC) solution with a weight ratio of 3:7. Additionally, 5 wt% fluoroethylene carbonate (FEC) was added to the mixture, which can contribute to the formation of a more stable solid electrolyte interphase (SEI). A total of 120 µL electrolyte was added to the electrode and separator. To ensure a homogeneous wettability of the electrodes with the liquid electrolyte, the electrodes were previously immersed in the electrolyte bath for 30 minutes. The cell components were assembled using an electric coin cell crimper (MSK-160D, MTI Corporation, Richmond, CA, USA). The galvanostatic measurements were performed at room temperature 22 °C applying a battery tester (BT 2000, Arbin Instruments, College Station, TX, USA). During formation, the half-cells with Si/C electrodes were discharged at a low constant current of 0.02C. A constant voltage was applied just after the cell reached the cutoff voltage of 0.01 V. Subsequently, the cells were charged at the same C-rate to upper cutoff voltage (1.5 V). The procedure was repeated for three cycles to ensure a homogenous SEI formation. After formation, the cells were prepared for the subsequent electrochemical C-rate performance analysis.

2.4 Laser-Induced Breakdown Spectroscopy

Laser-induced breakdown spectroscopy (LIBS) was performed on electrodes subsequently to electrochemical analysis, starting from the top of the composite layer towards the current collector. For this purpose a laser-induced plasma was

generated by a passive-mode-locked Nd:YAG laser (wavelength: 1064 nm, pulse length: 1.5 ns, pulse energy: 3 mJ, laser repetition rate: 100 Hz, focus diameter on sample 100µm) which was integrated in a LIBS analytic chamber system from Secopta GmbH, Germany. The plasma light of each laser ablation pulse was analyzed by a Czerny-Turner spectrometer (type: FiberLIBS SN013, Secopta GmbH, Teltow, Germany). The detector covers spectral ranges of 229 - 498 nm and 569 - 792 nm. The data were analyzed by SEC Viewer 1.9 (Secopta GmbH, Teltow, Germany). The intensities of the respective specific emission wavelengths of each element enable, overall, a complete quantitative or qualitative stoichiometric analysis of the electrode. Due to the effect of self-absorption at the wavelength of 670.77 nm, the Li^{I} emission wavelength of 610.35 nm was used for the analysis of lithium [14]. The calibration data were derived from LIBS and inductively coupled plasma atomic emission spectroscopy (ICP-OES) as described in [14]. Lithium concentration and distribution related to C-rates was systematically investigated in the structured and unstructured Si/C electrodes.

3. RESULTS AND DISCUSSION

3.5 Laser Structuring

The type of structured Si/C electrode is demonstrated in (Error! Reference source not found.**a** in the top view). Those electrodes are used for subsequent electrochemical performance studies. The structured channels in thick-film electrodes (> 70 µm) usually revealed a "V"-shaped contour. The channel widths on the top of the electrodes and in the middle were 21 ± 2 µm and 14.4 ± 1 µm, respectively, and its value is reduced to a few micrometers on the bottom of the channels which is close to the current collector. Model electrodes with micropillars were designed for the LIBS measurements to investigate the lithium diffusion pathway in structured electrodes. This special type of electrodes consists of micropillars with dimensions of 800 × 800 μm^2 (Error! Reference source not found.**b**), which are arranged with a periodicity of 1200 µm. The microcolumns are realized by direct ultrafast laser ablation of the electrode material around the micropillars. The layer thickness of the used electrodes is about 100 µm. A smooth copper surface reveals a successfully selective ablation without damaging the copper current collector.

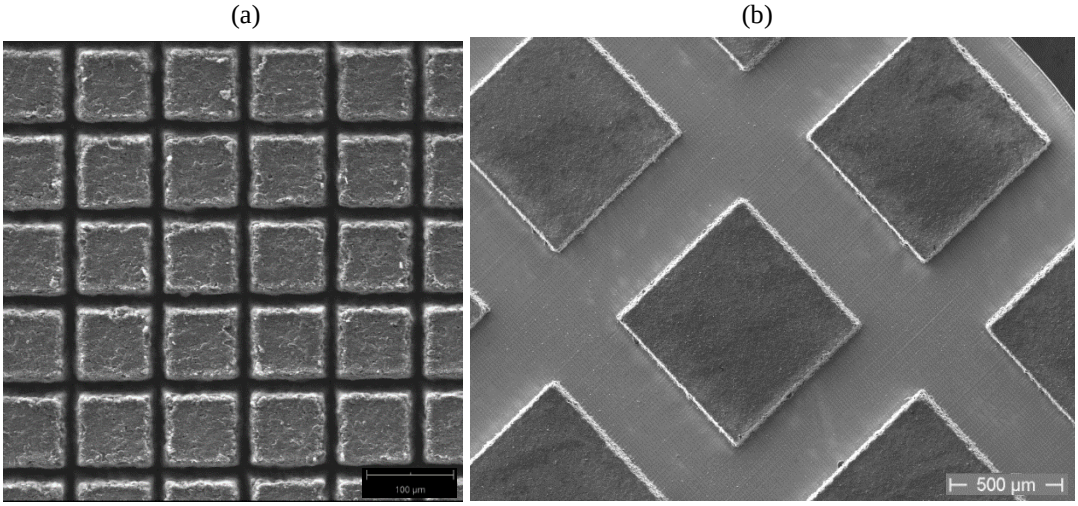

Figure 1:Scanning electron microscopy (SEM) images of (a) laser-generated grid structures with a period of 100 µm and (b) laser-generated model electrode with micropillar structures (800 µm × 800 µm).

3.6 Electrochemical Properties of Silicon-Based Electrodes

The phase change of graphite has already been studied in detail [15, 16]. Concerning the Si/C composite system, it was necessary to study the material property of silicon separately. Therefore, cyclic voltammetry (CV) was performed on the cells with thin composite silicon anodes consisting of 40 wt% silicon directly after the cell assembly. It is well known that the metastable crystalline phase $Li_{15}Si_4$ is only formed when the cutoff voltage is lower than a certain voltage value. Dahn et al. [17] reported that amorphous Si films crystallize below 0.03 V. Therefore a cut-off voltage of 0.01 V was applied (**Figure 2**).

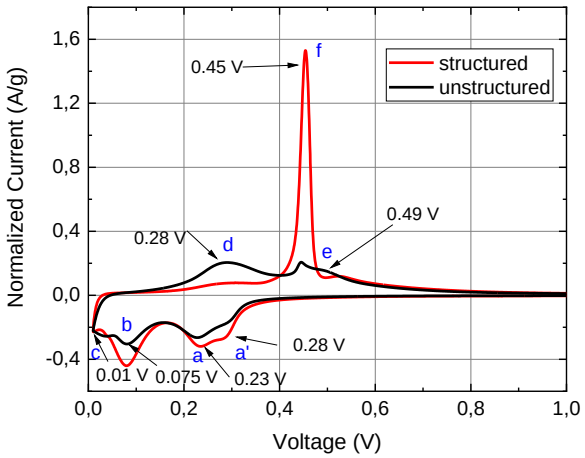

Figure 2: Cyclic voltammogram of cells with structured and unstructured Si electrodes recorded by a swap rate of 10 µV/s in a voltage window of 0.01–1.5 V.

The lithiation of silicon occurs for voltages lower than 0.3 V, e.g., a' at 0.28 V is marking the formation of the so-called P-I phase (LiSi) [18]. At 0.23 V the phase transition from P-I to P-II (a-Li_7Si_3) takes place. The broad current maximum at 0.075 V is assigned to the formation of the P-III phase (a-$Li_{3,16}Si$ [18] or a-$Li_{3.5}Si$ [19]). At a voltage of about 0.01 V the formation of cr-$Li_{15}Si_4$ is expected to occur [18, 20, 21]. The current peak at 0.45 V in the anodic reaction (delithiation) can be regarded as a material-specific indicator for the delithiation of cr-$Li_{15}Si_4$ phase which was previously formed at 0.01 V (cathodic reaction). The crystalline phase could be only detected in the laser-structured silicon electrodes. The obtained results indicated that compressive stress affected both the electrochemical potential and the kinetics of the electrochemical reaction. The CV experiments for unstructured Si electrode revealed that cutoff voltage is not the only condition for crystallization. Compressive stresses within the electrode can reduce the electrochemical potential and restrict the formation of the crystalline phase, namely, full lithiation.

Rate capability and cell degradation were studied for structured and unstructured Si/C electrodes. Grid structures with a pitch distance of 100 µm (Error! Reference source not found.**a**) were applied for structured electrodes. **Figure 3** show the selected results of the discharge capacity (lithiation of the Si/C electrode) as a function of cycle number.

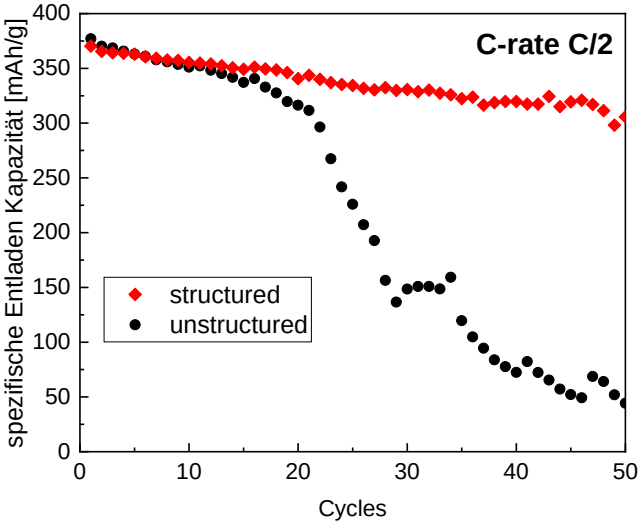

Figure 3: Specific discharge capacity of cells with structured and unstructured Si/C electrodes as function of cycle number.

This lifetime test exhibits that cells with unstructured electrodes show a significant drop in capacity at C/2 after already 20 cycles while cells with laser structured electrodes show a significant lifetime improvement due to a reduced mechanical degradation. Corresponding C-rate capability tests were performed [22]showing that the capacity of laser structured electrodes slightly decreased with increasing C-rate and could provide a capacity larger than 380 mAh/g at a C-rate of 2C. Subsequently, the capacity increased up to values larger of about 400 mAh/g at 0.1C indicating a slower capacity decay which is mainly attributed to chemical degradation and quality of the used silicon powders. For example the natural SiO_2 layer on the silicon particle's surface has an impact on the SEI formation and amount of irreversibly bonded lithium. However, for unstructured electrodes at C-rates equal or above 1C, a significant drop in capacity from about 200 mAg/h at 1C down to less than 100 mAh/g at 2C could be measured.

Kinetically limited lithium-ion diffusion is causing a lithium concentration gradient within the porous electrode which in turn negatively induces an impact on cell performances. Laser-induced breakdown spectroscopy (LIBS) is a perfect tool to identify such elemental gradients within the entire electrode. The LIBS studies of lithium distribution in structured and unstructured graphite and Si/C electrodes could prove that the 3D battery concept positively impacts the lithium-ion diffusion kinetics resulting in reduced cell polarization and extented cell life-time and rate capability. By means of LIBS it could be shown that due to laser structuring new lithium-ion diffusion pathways were generated. Lithium-ions preferably intercalate into the electrodes via the laser-generated sidewalls [23].

LIBS was performed with a point-to-point distance of 100 µm on Si/C electrodes after formation (C/20), and at an elevated C-rate of 1C for structured and unstructured electrodes. In case of delithiation, **Figure 4** shows the 2D lithium concentration profile of selected layers starting from the surface ("Layer 1"). The electrode material was ablated layer by layer down to the current collector.

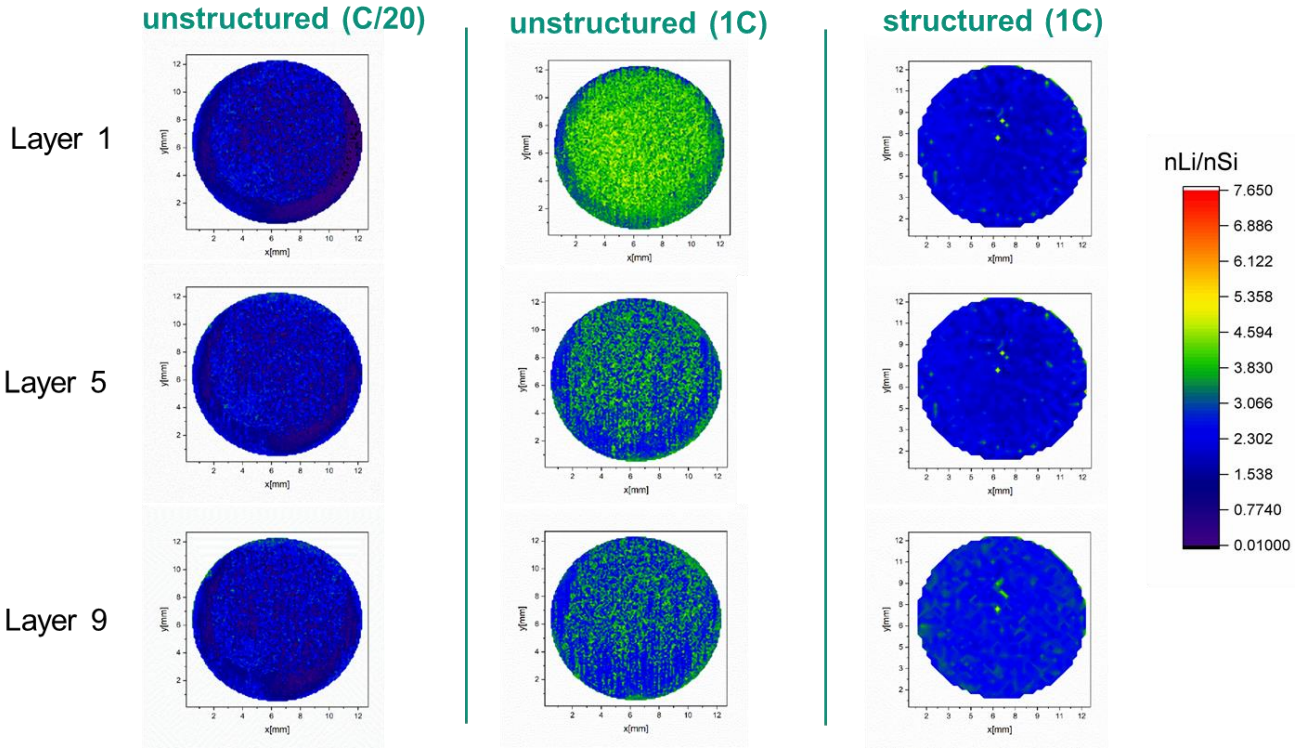

Figure 4: Lithium concentration profiles in structured and unstructured Si/C electrodes delithiated during formation (C/20) and at 1C. Electrode surface is assigned to "Layer 1". The average LIBS layer thickness takes 9 µm. The lithium concentration is defined as the ratio of the amount of Li substance to that of Si (nLi/nSi).

During formation (C/20) the lithium-ion diffusion kinetics is not a limiting factor which is shown by a homogenous and low lithium distribution even in the entire unstructured electrode. With increasing C-rate (1C) a significant inhomogeneity of lithium distribution in case of the unstructured electrode is detected. A lithium enrichment on the top of the unstructured electrode was measured. In the unstructured electrode, an overall average lithium concentration of 3.27 ± 0.75 was achieved. Due to the new diffusion pathways along the channel sidewalls, the lithium-ions could be efficiently extracted from the electrode material and revealed a lower average concentration of 2.70 ± 0.45. The residual lithium in the electrode,

which could not be completely extracted from the host material, led to the capacity fading at high C-rates. The process is particularly reversible, and the residual lithium in the electrode can be extracted by applying low C-rates.

In case of lithiation at 1C (not shown here), a lithium enrichment on top of the unstructured Si/C electrode within a depth of 40 µm was detected. Hereby, the average lithium concentration of the entire unstructured electrode took 3.38 which corresponds to a specific capacity of 212 mAh/g. The lithiation process was implemented gradually and locally from the top of the electrode down to the bottom. Contrary to this observation, the structured electrode revealed a higher average lithium concentration of 4.30 and a significantly enhanced homogenized lithium distribution in the entire electrode. This corresponds to a specific capacity of 272 mAh/g. Laser structuring shortened the diffusion path of the lithium-ions and reduced the overall cell impedance, which led to a significant increase in diffusion kinetics at high C-rates [22].

The achieved results indicate that laser-generated 3D electrodes can accelerate the lithium-ion transport during the lithiation and delithiation process and thereby realize the fast charging with reduced capacity loss. The lithium diffusion pathways established at a 1C were further investigated in detail using electrodes with micropillar structures (Error! Reference source not found.**b**) [22]. The measured lithium distribution showed that a lithium enrichment ($nLi/nSi > 6$) was formed along the contour of the micropillars. LIBS results indicate that at elevated C-rates lithium-ions prefer to diffuse through the free electrolyte via laser-generated sidewalls. This is due to the lithium-ion mobility in free electrolyte which is faster than in the composite electrode affected by porosity and tortuosity. In addition, the 3D topology of composite electrodes contributes to the formation of new lithium-ion diffusion pathways. However, in contrast to the LIBS results obtained for graphite electrodes [23], a significant lower lithium concentration ($nLi/nSi \approx 3,4$) was detected on top of the electrode. This is attributed to the closure of pores within the separator and compressive pressure in the electrodes caused by the volume expansion of silicon. The lithiation process can be restricted by mechanical compressive stress. The electrode materials along the sidewalls are almost free from mechanical loads. Therefore, the lithiation, in particular the lithiation in silicon, was effectively promoted there.

4. CONCLUSION

In the presented paper, the high rate capability and cycle stability of cells with structured and unstructured Si/C electrodes was presented. The influence of degradation processes in Si/C electrodes was correlated with regard to the lithium concentration profiles in the entire electrodes. The lithium concentration and distribution of the structured electrodes showed that at increased C-rates, new lithium-ion diffusion pathways were established in the composite electrodes along the laser-generated sidewalls. The observed effect was due to a low compressive stress in the active material along the sidewalls and a high lithium-ion mobility in the free electrolyte compared to the electrolyte embedded in the porous composite electrode. Cell degradation of Si/C electrodes was attributed to the trapped lithium in the Si/C electrode. It can be concluded that the mechanical stress accelerates chemical degradation and leads to early cell failure. 3D Si/C electrode architectures established by ultrafast laser ablation enable a high rate capability, accelerate the lithium-ion transport, and can effectively reduce mechanical stress and cell degradation. All these advantages can push silicon-based electrodes beyond the state of the art into a high-energy anode material for next-generation batteries.

5. ACKNOWLEDGEMENTS

We are grateful to Thomas Bergfeldt at Karlsruhe Institute of Technology for the chemical analysis by inductively coupled plasma-optical emission spectrometry as well as Danni Yin for the implementation of LIBS measurements and Yuanchun Huang for technical assistance and the evaluation of battery measurements. This research was funded by German Research Foundation (DFG, project no. 392322200).

6. REFERENCES

1. Dühnen, S., J. Betz, M. Kolek, R. Schmuch, M. Winter, and T. Placke, *Toward green battery cells: perspective on materials and technologies.* Small Methods, 2020. 4(7): p. 2000039.
2. Nykvist, B. and M. Nilsson, *Rapidly falling costs of battery packs for electric vehicles.* Nature climate change, 2015. 5(4): p. 329-332.
3. Wood III, D.L., J. Li, and C. Daniel, *Prospects for reducing the processing cost of lithium ion batteries.* Journal of Power Sources, 2015. 275: p. 234-242.

4. Mauler, L., F. Duffner, W.G. Zeier, and J. Leker, *Battery cost forecasting: a review of methods and results with an outlook to 2050.* Energy & Environmental Science, 2021. 14: p. 4712-4739.
5. Andre, D., S.-J. Kim, P. Lamp, S.F. Lux, F. Maglia, O. Paschos, and B. Stiaszny, *Future generations of cathode materials: an automotive industry perspective.* Journal of Materials Chemistry A, 2015. 3(13): p. 6709-6732.
6. Liu, J., Z. Bao, Y. Cui, E.J. Dufek, J.B. Goodenough, P. Khalifah, Q. Li, B.Y. Liaw, P. Liu, and A. Manthiram, *Pathways for practical high-energy long-cycling lithium metal batteries.* Nature Energy, 2019. 4(3): p. 180-186.
7. Tarascon, J.M. and M. Armand, *Issues and challenges facing rechargeable lithium batteries.* Nature, 2001. 414(6861): p. 359-367.
8. Tariq, F., V. Yufit, D.S. Eastwood, Y. Merla, M. Biton, B. Wu, Z. Chen, K. Freedman, G. Offer, and E. Peled, *In-operando X-ray tomography study of lithiation induced delamination of Si based anodes for lithium-ion batteries.* ECS Electrochemistry Letters, 2014. 3(7): p. A76.
9. Obrovac, M.N. and L.J. Krause, *Reversible Cycling of Crystalline Silicon Powder.* Journal of The Electrochemical Society, 2007. 154(2): p. A103.
10. Kwade, A., W. Haselrieder, R. Leithoff, A. Modlinger, F. Dietrich, and K. Droeder, *Current status and challenges for automotive battery production technologies.* Nature Energy, 2018. 3(4): p. 290-300.
11. Schmuch, R., R. Wagner, G. Hörpel, T. Placke, and M. Winter, *Performance and cost of materials for lithium-based rechargeable automotive batteries.* Nature Energy, 2018. 3(4): p. 267-278.
12. Pfleging, W., *Recent Progress in Laser Texturing of Battery Materials: A Review of Tuning Electrochemical Performances, Related Material Development, and Prospects for Large-Scale Manufacturing.* International Journal of Extreme Manufacturing, 2020. 3: p. 1.
13. Zheng, Y., H. Seifert, H. Shi, Y. Zhang, C. Kübel, and W. Pfleging, *3D silicon/graphite composite electrodes for high-energy lithium-ion batteries.* Electrochimica Acta, 2019. 317: p. 502-508.
14. Smyrek, P., J. Pröll, H. Seifert, and W. Pfleging, *Laser-induced breakdown spectroscopy of laser-structured Li (NiMnCo) O2 electrodes for lithium-ion batteries.* Journal of the Electrochemical Society, 2015. 163(2): p. A19.
15. Levi, M., E. Levi, and D. Aurbach, *The mechanism of lithium intercalation in graphite film electrodes in aprotic media. Part 2. Potentiostatic intermittent titration and in situ XRD studies of the solid-state ionic diffusion.* Journal of Electroanalytical Chemistry, 1997. 421(1-2): p. 89-97.
16. Levi, M.D. and D. Aurbach, *The mechanism of lithium intercalation in graphite film electrodes in aprotic media. Part 1. High resolution slow scan rate cyclic voltammetric studies and modeling.* Journal of Electroanalytical Chemistry, 1997. 421(1-2): p. 79-88.
17. Hatchard, T. and J. Dahn, *In situ XRD and electrochemical study of the reaction of lithium with amorphous silicon.* Journal of The Electrochemical Society, 2004. 151(6): p. A838.
18. Datta, M.K. and P.N. Kumta, *In situ electrochemical synthesis of lithiated silicon–carbon based composites anode materials for lithium ion batteries.* Journal of Power Sources, 2009. 194(2): p. 1043-1052.
19. Li, J. and J. Dahn, *An in situ X-ray diffraction study of the reaction of Li with crystalline Si.* Journal of The Electrochemical Society, 2007. 154(3): p. A156.
20. Reyes Jiménez, A., R. Klöpsch, R. Wagner, U.C. Rodehorst, M. Kolek, R. Nölle, M. Winter, and T. Placke, *A Step toward High-Energy Silicon-Based Thin Film Lithium Ion Batteries.* ACS Nano, 2017. 11(5): p. 4731-4744.
21. Baggetto, L., R.A.H. Niessen, F. Roozeboom, and P.H.L. Notten, *High Energy Density All-Solid-State Batteries: A Challenging Concept Towards 3D Integration.* Advanced Functional Materials, 2008. 18(7): p. 1057-1066.
22. Zheng, Y., D. Yin, H.J. Seifert, and W. Pfleging, *Investigation of Fast-Charging and Degradation Processes in 3D Silicon–Graphite Anodes.* Nanomaterials, 2021. 12(1): p. 140.
23. Zheng, Y., L. Pfäffl, H.J. Seifert, and W. Pfleging, *Lithium distribution in structured graphite anodes investigated by laser-induced breakdown spectroscopy.* Applied Sciences, 2019. 9(20): p. 4218.